

# Vitamin B<sub>12</sub> Derivative Enables Cobalt-Catalyzed Atom Transfer Radical Polymerization

Sajjad Dadashi-Silab, Cristina Preston-Herrera, and Erin E. Stache\*



Cite This: *J. Am. Chem. Soc.* 2023, 145, 19387–19395



Read Online

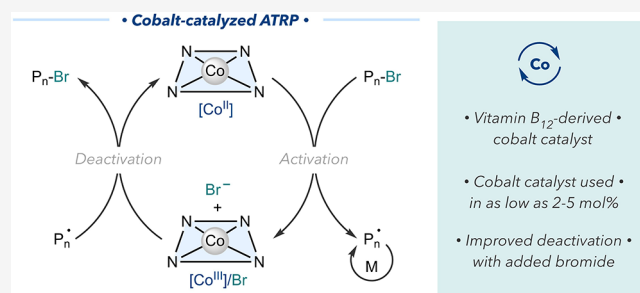
ACCESS |

Metrics & More

Article Recommendations

Supporting Information

**ABSTRACT:** Advances in controlled radical polymerizations by cobalt complexes have primarily taken advantage of the reactivity of cobalt as a persistent radical to reversibly deactivate propagating chains by forming a carbon–cobalt bond. However, cobalt-mediated radical polymerizations require stoichiometric ratios of a cobalt complex, deterring its utility in synthesizing well-defined polymers. Here, we developed a strategy to use cobalt as a catalyst to control radical polymerizations via halogen atom transfer with alkyl halide initiators. Using a modified, hydrophobic analogue of vitamin B<sub>12</sub> (heptamethyl ester cobyrinate) as a cobalt precatalyst, we controlled the polymerization of acrylate monomers. The polymerization efficiency of the cobalt catalyst was significantly improved by additional bromide anions, which enhanced the deactivation of propagating radicals yielding polymers with dispersity values <1.2 using catalyst concentrations as low as 5 mol %. We anticipate that the development of cobalt catalysis in atom transfer radical polymerization will enable new opportunities in designing catalytic systems for the controlled synthesis of polymers.



Downloaded via CORNELL UNIV on October 23, 2023 at 17:55:44 (UTC).  
See https://pubs.acs.org/sharingguidelines for options on how to legitimately share published articles.

high concentrations of metal complexes limit their application in synthesizing well-defined polymers.

In contrast, atom transfer radical polymerization (ATRP) typically uses copper catalysts to activate alkyl halide initiators and generate radicals. The reversible transfer of halogen atoms to propagating radicals by the oxidized form of the catalyst deactivates polymer chains, establishing the ATRP equilibrium.<sup>16–19</sup> The exceptional ability of copper complexes to mediate ATRP reactions has led to tremendous advances in synthesizing well-defined polymeric materials.<sup>20</sup> In this regard, the development of new classes of ATRP catalysts offers the discovery of novel chemical reactivities for materials design and sustainable catalysis.<sup>21–25</sup>

Despite the excellence of cobalt in controlling radical polymerizations via the organometallic pathway, its reactivity in catalyzing atom transfer processes remains elusive. Attempts to use cobalt complexes under ATRP conditions have shown a limited degree of control over polymerization with poor initiator efficiency, even in the presence of stoichiometric amounts of the cobalt catalysts concerning the initiator.<sup>26–30</sup> We hypothesized whether designing new catalytic approaches

Received: June 27, 2023

Published: August 22, 2023



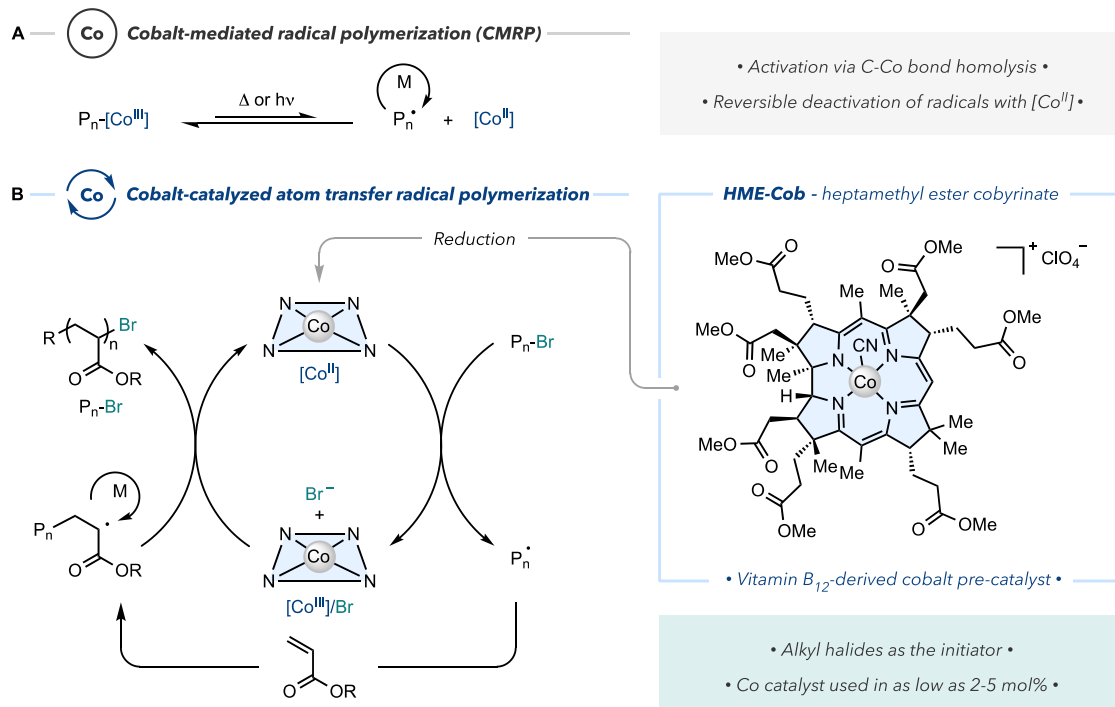
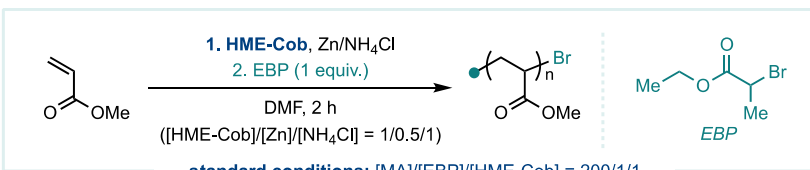


**Figure 1.** Use of cobalt in controlled radical polymerization reactions. (A) Cobalt-mediated radical polymerization, where the deactivation of propagating radicals by the persistent radical ( $Co^{II}$ ) affords cobalt-containing polymer chains in the dormant state. (B) Our proposed strategy to use a vitamin  $B_{12}$ -derived cobalt complex (HME-Cob) as a catalyst in controlled radical polymerization enabled via a halogen atom transfer mechanism.

**Table 1. Cobalt-Catalyzed Polymerization of MA<sup>a</sup>**



standard conditions:  $[MA]/[EBP]/[HME-Cob] = 200/1/1$

entry	conditions	temp (°C)	conv. (%)	$M_{n,th}$	$M_n$	$D$	$I_{eff} (%)$
1	all	40	57	10,000	8150	1.20	123
2	no Co	40	0				
3	no Zn	40	0				
4	all + TEMPO	40	0				
5	$[Co] = 0.50$ equiv.	60	88	15,100	10,300	1.35	145
6	$[Co] = 0.20$ equiv.	60	83	14,300	10,300	1.63	139
7	$[Co] = 0.10$ equiv.	60	66	11,500	13,100	1.93	88
8	$[Co] = 0.05$ equiv.	60	43	7600	17,100	2.03	45

<sup>a</sup>The cobalt catalyst was reduced by Zn before polymerization under the conditions:  $[HME-Cob]/[Zn]/[NH_4Cl] = 1/0.5/1$  followed by the addition of the alkyl halide to initiate the polymerization. Theoretical molecular weight,  $M_{n,th} = ([MA]/[EBP] \times conv.) + M_{EBP}$ . Experimental molecular weight,  $M_n$ , measured by the refractive detector GPC with a refractive index detector relative to polystyrene standards. Initiator efficiency,  $I_{eff} = M_{n,th}/M_n$ .

would impart efficient atom transfer reactivity for cobalt in mediating controlled radical polymerization reactions. The majority of the cobalt complexes that perform as an OMRP mediator feature a dianionic ligand framework such as porphyrins, salens, or acetylacetones.<sup>10,11</sup> We wondered whether structural alteration of the cobalt complex by using

a monoanionic ligand framework such as corrin would provide access to different electronic properties and reactivity for controlling polymerization reactions.

Cobalt complexes, including vitamin  $B_{12}$  and its hydrophobic derivatives, have been used in various catalytic, small-molecule transformations.<sup>31-36</sup> The reduced form of the cobalt

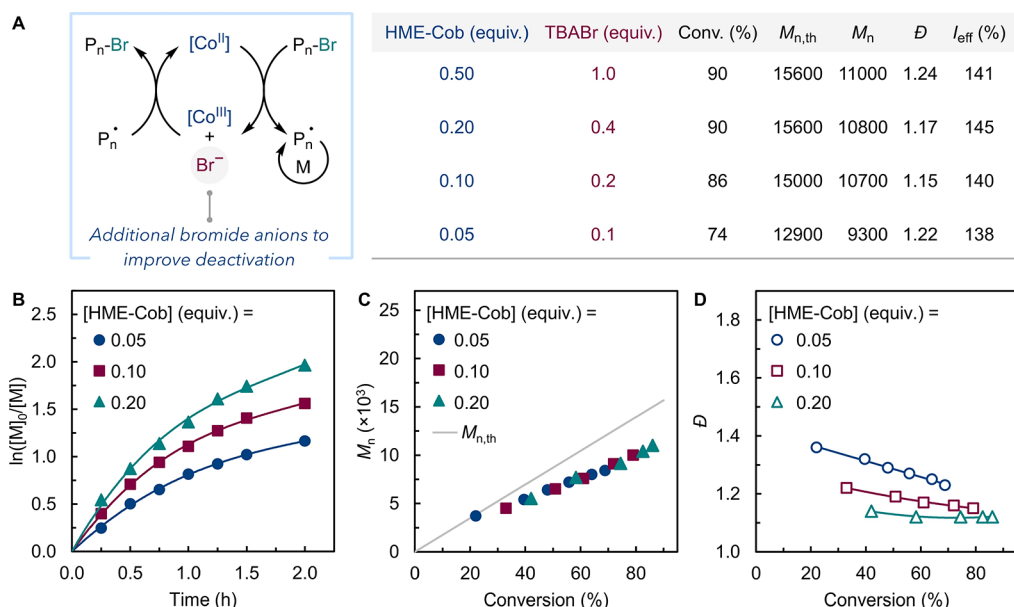


**Figure 2.** (A) Cobalt-catalyzed polymerization of MA in the presence of additional bromide anions to improve the deactivation of propagating radicals and control over polymerization. (B) Kinetics of the polymerization of MA using 0.05, 0.10, and 0.20 equiv of the cobalt catalyst (with 0.10, 0.20, and 0.40 equiv of TBABr, respectively). (C) Evolution of the number average molecular weight ( $M_n$ , solid points) and (D) dispersity ( $D$ , empty points) per monomer conversion. Reaction conditions:  $[MA]/[EBP]/[HME\text{-Cob}] = 200/1/x$  ( $x = 0.05\text{--}0.50$ ) in DMF (50 vol %) at 60 °C;  $[HME\text{-Cob}]/[Zn]/[NH_4Cl] = 1/0.5/1$ .

complexes possess nucleophilic reactivity that enables their reaction with alkyl halides to form carbon-based radicals via nucleophilic substitution or electron transfer mechanisms. Using a hydrophobic analogue of vitamin B<sub>12</sub>, Gryko and co-workers reported cobalt-catalyzed atom transfer radical addition for the functionalization of alkenes using the supernucleophile  $Co^I$  to generate alkyl radicals.<sup>37</sup> Inspired by this reactivity of cobalt, we designed a strategy to mediate a controlled radical polymerization using cobalt complexes as the catalyst. We demonstrate that both the  $Co^I$  and  $Co^{II}$  forms of the cobyrinate complex can be accessed for alkyl halide activation, with the  $Co^{II}$  complex providing a higher degree of control over polymerization through a  $Co^{II}/Co^{III}$  redox cycle enabling an efficient atom transfer mechanism (Figure 1B). Similar to ATRP reactions, we posit that control over polymerization is attained via halogen atom transfer to cap propagating radicals by the oxidized cobalt complex, completing the catalytic cycle. We show that the polymerization reactivity of cobalt can be selectively switched from the organometallic to an atom transfer mechanism by altering its ligand framework under ATRP-promoting conditions. Here, a vitamin B<sub>12</sub>-derived cobalt complex offered efficient and selective atom transfer reactivity instead of undergoing the organometallic pathway.

## RESULTS AND DISCUSSION

Modification of vitamin B<sub>12</sub> (cyanocobalamin) to a hydrophobic analogue, heptamethyl ester cobyrinate (HME-Cob), allows for its solubility and use as a catalyst in organic media.<sup>38</sup> The catalytic efficiency of the cobalt complex was examined in the polymerization of methyl acrylate (MA) using ethyl 2-bromopropionate (EBP) as the initiator in *N,N*-dimethylformamide (DMF). The HME-Cob catalyst was activated by reduction with zinc and ammonium chloride ( $NH_4Cl$ ) before polymerization. In the presence of a stoichiometric amount of cobalt complex, with respect to EBP, polymerization of MA

reached 57% monomer conversion in 2 h, showing controlled molecular weight and a low dispersity of 1.20 (Table 1, entry 1). No polymerization of MA was observed in the absence of either the cobalt complex or the zinc reductant (Table 1, entries 2 and 3), indicating the importance of the reduced form of the catalyst to activate the polymerization. Furthermore, the addition of 2,2,6,6-tetramethylpiperidine-1-oxyl (TEMPO) as a radical scavenger prevented monomer conversion proving the radical nature of the polymerization (Table 1, entry 4).

Decreasing the concentration of the cobalt catalyst resulted in a decrease in the polymerization efficiency and diminished control over molecular weight and dispersity (Table 1, entries 5–8, and Figure S5). Even though increasing the temperature from 40 to 60 °C provided higher monomer conversions, polymerization control was still poor (Figures S5 and S6). In the presence of 50 mol % (0.5 equiv with respect to the initiator) of HME-Cob, the dispersity of the resulting polymer increased to 1.35. Further decreasing the catalyst concentration led to higher dispersity values at 5 mol % cobalt catalyst loading, as the resulting polymer showed a dispersity of 2.03 (Table 1, entry 8). Additionally, limited monomer conversion and low initiator efficiencies were observed at reduced catalyst concentrations, indicating inefficient activation/deactivation of polymer chains.

**Addition of Bromide.** Considering the proposed mechanism that involves the reversible transfer of bromine to polymer chains during the deactivation step (Figure 1B), we hypothesized that additional bromide anions could enhance the deactivation of propagating radicals. The effect of additional bromide ions has been proved in copper-catalyzed ATRP reactions in water to promote deactivation by preventing the dissociation of the deactivator species ( $Cu^{II}\text{-}Br$ ) to  $Cu^{II}$  and Br ions.<sup>39</sup> Accordingly, we improved polymerization efficiency and control over molecular weight using additional tetrabutylammonium bromide (TBABr), enhancing the deactivation step (Figures 2A, S7, and S8).

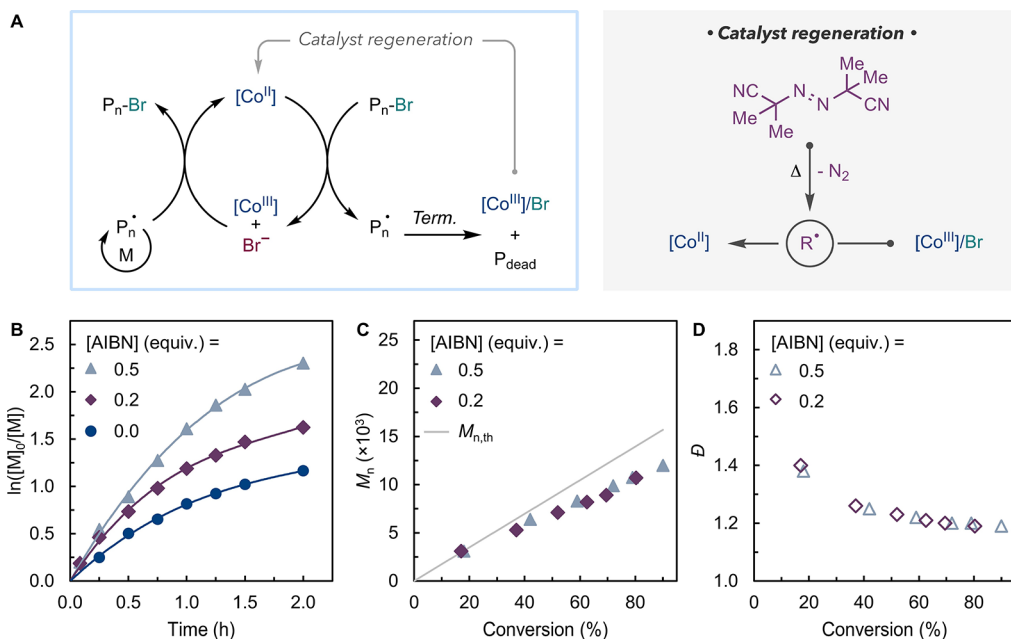


**Figure 3.** (A) Cobalt-catalyzed ATRP with catalyst regeneration using AIBN to compensate for converting the activator catalyst to deactivator species because of radical termination reactions. (B) Kinetics of the polymerization of MA using 0.05 equiv of the cobalt catalyst in the presence of additional AIBN (0.0, 0.2 and 0.5 equiv). (C) Evolution of the number average molecular weight ( $M_n$ , solid points) and (D) dispersity ( $D$ , empty points) per monomer conversion. Reaction conditions:  $[\text{MA}]/[\text{EBP}]/[\text{HME-Cob}]/[\text{TBABr}]/[\text{AIBN}] = 200/1/0.05/0.10/x$  ( $x = 0, 0.2$ , or  $0.5$  equiv) in DMF (50 vol %) at  $60^\circ\text{C}$ .

The polymerization efficiency increased in the presence of additional bromide anions affording high monomer conversions and polymers with low dispersity values ( $\sim 1.2$ ) at reduced catalyst concentrations (5–50 mol %). This observation may further suggest that under these conditions, the deactivation occurs via an outer-sphere process requiring a termolecular reaction involving the propagating radical, oxidized cobalt catalyst, and the bromide anion.

**Kinetic Studies.** Kinetic analysis of the polymerization showed an increase in the overall rate by increasing the concentration of the cobalt catalyst from 5 to 10 and 20 mol % (Figure 2B). The resulting polymers showed controlled molecular weights in agreement with theoretical values and low dispersity (Figure 2C,D).

We observed the rate decrease as the polymerization progressed to higher monomer conversions, deviating from the linear first-order kinetics (Figure 2B). This decrease in the rate of polymerization can be attributed to irreversible radical termination reactions that convert the activator catalyst ( $\text{Co}^{II}$ ) to the deactivator species (i.e.,  $\text{Co}^{III}/\text{Br}$ ), ultimately impeding the progress of polymerization (Figure 2A). To mitigate this problem, we employed a catalyst regeneration approach to drive the polymerization forward by continuously reducing the oxidized form of the catalyst to the activator species *in situ*.<sup>40</sup> Using azobisisobutyronitrile (AIBN) as a radical source for catalyst regeneration in a process similar to initiators for continuous activator regeneration (ICAR) ATRP,<sup>39,40</sup> polymerization of MA in the presence of 5 mol % of Co showed enhanced kinetics providing high monomer conversions ( $>80$ –90% in 2 h, Figure 3B). Control over polymerization was maintained, with molecular weights increasing as a function of monomer conversion while providing low dispersity values (Figure 3C,D).

With catalyst regeneration using AIBN, we further attempted to decrease the concentration of the cobalt catalyst

to 1–2 mol % while still obtaining high monomer conversions. However, in ATRP reactions, the rate of deactivation and control over dispersity depends on the total concentration of the deactivator species (i.e.,  $\text{Co}^{III}/\text{Br}$ ). Therefore, decreasing the catalyst loading afforded polymers with higher dispersity values. For example, polymerization of MA using 2 mol % of HME-Cob in the presence of 0.5 equiv AIBN reached 86% monomer conversion in 2 h with a dispersity of 1.33 (Figures S15 and S16). The high polymerization efficiency achieved using only 2 mol % of the cobalt catalyst signifies its excellence and potential for catalyzing polymerization reactions.

Importantly, we observed similar initiator efficiencies for polymerizations under different concentrations of the cobalt catalyst that supports the prevalence of the ATRP mechanism where polymer chains are capped with bromine. Upon changing the concentration of the alkyl halide initiator, we were able to synthesize polymers with varying degrees of polymerization (DP = 100–800) and molecular weights in a controlled manner regardless of the catalyst concentration (Figure S17). This observation contrasts with the OMRP systems that afford cobalt-capped polymers whose target molecular weight depends on the concentration of the cobalt complex relative to the monomer. Structural analysis of the resulting polymers by  $^1\text{H}$  NMR spectroscopy confirmed the presence of bromine chain end functionality (Figure S3) obtained under these conditions. The molecular weight of the polymers was measured by gel-permeation chromatography (GPC) equipped with a refractive index detector relative to polystyrene standards. As a result, the experimental molecular weights were lower than theoretical values giving initiator efficiencies typically  $\sim 130$ –140%. We calculated the degree of polymerization and molecular weight of the polymers by NMR chain-end analysis, which showed values in agreement with the theoretical molecular weights, confirming near-quantitative initiator efficiency  $\sim 107\%$  (Figure S3).

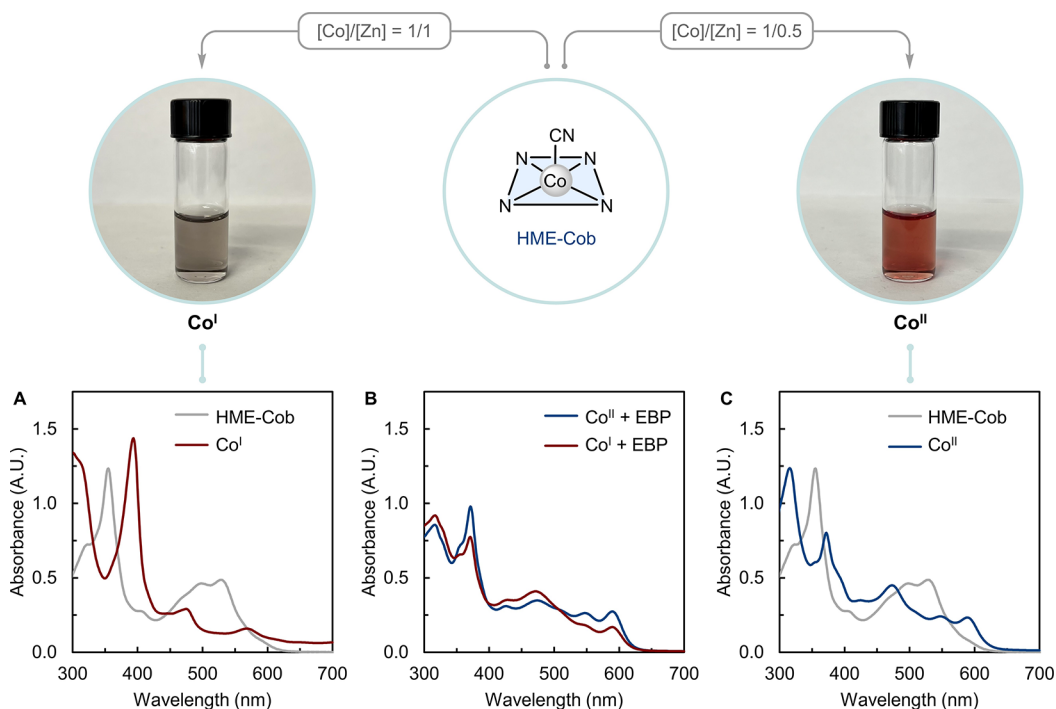
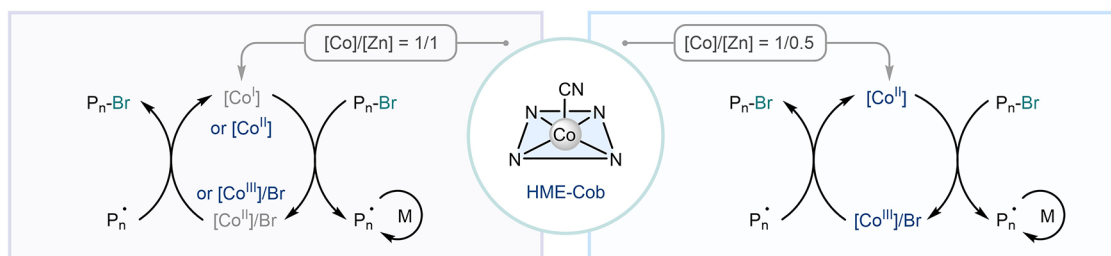


**Figure 4.** Reduction of HME-Cob by Zn (and  $\text{NH}_4\text{Cl}$ ) to generate either  $\text{Co}^{\text{I}}$  or  $\text{Co}^{\text{II}}$  complexes using a 1/1 or 1/0.5 ratio of Co to Zn, respectively. (A and C) UV-vis spectra of HME-Cob and  $\text{Co}^{\text{I}}$  complex (with 1 equiv of Zn with respect to Co) and that of  $\text{Co}^{\text{II}}$  complex (with 0.5 equiv of Zn with respect to Co), respectively. (B) UV-vis spectra of the reduced Co complexes followed by adding the alkyl halide initiator, EBP. For UV-vis measurements,  $[\text{Co}] = 50 \mu\text{M}$  in DMF.



Entry	TBABr (equiv.)	Conv. (%)	$M_{n,\text{th}}$	$M_n$	$\mathcal{D}$	$I_{\text{eff}} (\%)$	Entry	TBABr (equiv.)	Conv. (%)	$M_{n,\text{th}}$	$M_n$	$\mathcal{D}$	$I_{\text{eff}} (\%)$
1	0.00	52	9000	16400	1.91	55	7	0.00	43	7600	17100	2.03	45
2	0.01	57	10000	12500	1.88	80	8	0.01	70	12300	9800	1.70	125
3	0.02	62	10800	11900	1.77	91	9	0.02	73	12800	10400	1.49	123
4	0.05	64	11200	9900	1.60	123	10	0.05	62	10800	7500	1.33	144
5	0.10	70	12200	8700	1.46	140	11	0.10	74	12900	9300	1.22	138
6	0.20	72	12500	8500	1.35	147	12	0.20	58	10100	7900	1.22	128

$[\text{MA}]/[\text{EBP}]/[\text{HME-Cob}]/[\text{Zn}]/[\text{NH}_4\text{Cl}] = 200/1/0.05/0.05/0.10$

$[\text{MA}]/[\text{EBP}]/[\text{HME-Cob}]/[\text{Zn}]/[\text{NH}_4\text{Cl}] = 200/1/0.05/0.025/0.05$

**Figure 5.** Comparison of the polymerization efficiency of the cobalt catalyst initiated by  $\text{Co}^{\text{I}}$  (entries 1–6, using a 1/1 ratio of Co to Zn) or  $\text{Co}^{\text{II}}$  (entries 7–12, using a 1/0.5 ratio of Co to Zn) complexes, respectively. The polymerization of MA was conducted using 0.05 equiv (5 mol % with respect to EBP) of the cobalt catalyst in the presence of a varying ratio of additional bromide anion (TBABr) in DMF (50 vol %) at 60 °C for 2 h.

**Initiation via  $\text{Co}^{\text{II}}$  vs  $\text{Co}^{\text{I}}$ .** The versatility of cobalt chemistry allowed accessing HME-Cob-based complexes with different oxidation states ( $\text{Co}^{\text{I}}$  and  $\text{Co}^{\text{II}}$ ) therefore, examining their efficiency in initiating polymerization reactions. The HME-Cob complex was reduced to either  $\text{Co}^{\text{II}}$  or  $\text{Co}^{\text{I}}$  using 0.5 or 1 equiv of Zn (relative to Co), respectively (Figure 4). The  $\text{Co}^{\text{I}}$  complex formed a dark gray/metallic solution in DMF,

whose UV-vis spectra showed the disappearance of the  $\alpha$  and  $\beta$  absorption bands in the 450–550 nm region that are typical features of the coordination of axial ligands in HME-Cob (Figure 4A and top-left). In addition, the UV-vis spectra of the  $\text{Co}^{\text{I}}$  complex showed a strong absorption peak corresponding to the  $\gamma$  band centered at ~390 nm, consistent with literature reports.<sup>41,42</sup> The reduction of HME-Cob to  $\text{Co}^{\text{II}}$

using 0.5 equiv of Zn formed a brown/orange solution in DMF with spectral features appearing in the 500–600 nm region (Figure 4C and top-right). We attribute these features to the presence of a coordinating ligand at the axial position, which red-shifted compared to HME-Cob as the complex was reduced to  $\text{Co}^{\text{II}}$ .

Examining the catalytic efficiency of  $\text{Co}^{\text{I}}$  and  $\text{Co}^{\text{II}}$  complexes revealed different behavior in the initiation and the ability of these complexes to assert control over polymerization. We studied the effect of additional bromide anions on polymerization efficiency initiated by  $\text{Co}^{\text{I}}$  or  $\text{Co}^{\text{II}}$ . In both complexes (using 5 mol % with respect to EBP), increasing the concentration of TBABr from 0 to 20 mol % led to higher initiator efficiencies and lower dispersity values, indicating improved control over polymerization. For instance, polymerization of MA initiated by  $\text{Co}^{\text{I}}$  in the presence of 10 or 20 mol % of additional TBABr resulted in polymers with dispersity values of 1.46 or 1.35, respectively (Figure 5, entries 5 and 6). In contrast, polymerizations initiated by the  $\text{Co}^{\text{II}}$  complex showed lower dispersity values than those initiated by  $\text{Co}^{\text{I}}$ . For example, in the presence of 10 or 20 mol % of additional TBABr, the resulting polymers initiated by  $\text{Co}^{\text{II}}$  both showed a dispersity of 1.22 (Figure 5, entries 11 and 12).

The differences in polymerization efficiency reflect the different reactivity of the  $\text{Co}^{\text{I}}$  and  $\text{Co}^{\text{II}}$  complexes. The reaction of  $\text{Co}^{\text{I}}$  with the alkyl halide initiator could undergo an electron transfer to form propagating radicals while oxidizing the complex to  $\text{Co}^{\text{II}}$ . Alternatively, due to the high nucleophilicity of  $\text{Co}^{\text{I}}$ , a nucleophilic substitution with alkyl halides may well be feasible to generate organocobalt species ( $\text{Co}^{\text{III}}\text{-R}$ ) that ultimately can homolyze to form radicals and  $\text{Co}^{\text{II}}$ . We hypothesize that because the reduction of  $\text{Co}^{\text{II}}$  to  $\text{Co}^{\text{I}}$  is energetically demanding and less favorable by the propagating radicals, the deactivation of polymerization may not be efficient via bromine atom transfer by  $\text{Co}^{\text{II}}$ . This hypothesis is supported by the UV-vis spectroscopic analysis of the  $\text{Co}^{\text{I}}$  solution, which rapidly reacted with the alkyl halide and oxidized to  $\text{Co}^{\text{II}}$  without the reformation of  $\text{Co}^{\text{I}}$  (Figure 4B).

Based on these observations, we propose that upon the reaction of  $\text{Co}^{\text{I}}$  with the initiator, the catalyst is oxidized to  $\text{Co}^{\text{II}}$ , which can undergo further reaction to activate alkyl halides via electron transfer forming a  $\text{Co}^{\text{III}}$  complex. Subsequently, the  $\text{Co}^{\text{III}}$  complex can act as an efficient deactivator of propagating radicals in the presence of bromide anions. Therefore, when initiated by  $\text{Co}^{\text{I}}$ , we assume that the deactivator complex is not formed in the first step of the activation. As a result, polymer chains can grow nonuniformly. Even though  $\text{Co}^{\text{I}}$  initiates the polymerization, it is more likely that the equilibrium follows a redox process between  $\text{Co}^{\text{II}}$  and  $\text{Co}^{\text{III}}$  complexes instead of  $\text{Co}^{\text{I}}$  and  $\text{Co}^{\text{II}}$  as the activator and deactivator species, respectively. This contrasts with initiation using a  $\text{Co}^{\text{II}}$  complex where the activation and deactivation steps can be efficiently established and sustained to control the polymerization and afford polymers with low dispersity values.

**Chain Extension Experiments.** We performed *in situ* chain extension experiments to demonstrate the high chain-end fidelity of polymers obtained by cobalt catalysis. A poly(methyl acrylate) (PMA) macroinitiator was synthesized using 5 mol % of the cobalt catalyst in the presence of AIBN for catalyst regeneration. Conversion of MA reached >95% ( $M_n = 11,300$  and  $D = 1.19$ ), allowing the *in situ* chain extension without purification of the macroinitiator. The addition of the (2-methoxyethyl) acrylate (MEA) monomer

resulted in the formation of the block copolymer, PMA-*b*-PMEA, as evident in the GPC analysis where the molecular weight increased to 32,000 with a dispersity of 1.26. The GPC trace of the resulting copolymer shifted to a higher molecular weight showing only negligible unreacted macroinitiator, which confirms the high chain end functionality of polymers (Figure 6).

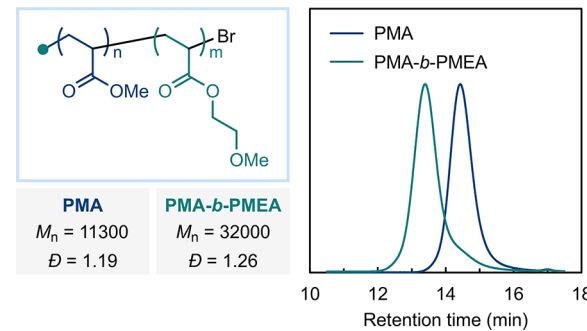


**Figure 6.** Block copolymerization experiment with PMA-*b*-PMEA demonstrating high chain end functionality of polymers synthesized under cobalt-catalyzed ATRP.

**Alkyl Halide Initiators.** A series of activated alkyl bromide initiators with ester, benzyl, or nitrile stabilizing groups were successfully used to polymerize MA (Figures 7A and S21–S24). For example, controlled polymerization of MA was successfully initiated using a tertiary alkyl bromide initiator (ethyl  $\alpha$ -bromo isobutyrate, EBiB). The tertiary nature of this initiator may further suggest that the activation by  $\text{Co}^{\text{II}}$  occurs via an electron transfer as opposed to the nucleophilic substitution mechanisms.

While both benzyl bromide (BnBr) and bromopropionitrile (BPN) provided efficient polymerization of MA, the use of bromoacetonitrile (BAN) failed to initiate the polymerization. We attribute this observation to the primary nature of BAN being less activated than its secondary analogue, BPN. We further studied the effect of the halogen in the initiator and the nature of added halide source. In contrast to the bromine-based initiators, alkyl chloride initiator (ethyl 2-chloropropionate, ECP) showed poor initiation efficiency and limited monomer conversion (Figure S25). The high dissociation energy of the C–Cl bond may hinder the fast and efficient activation of the alkyl chlorides by the cobalt catalyst, therefore, giving poor control over polymerization. In addition, we examined the effect of additional chloride anions in the polymerization of MA by the cobalt catalyst. Using a bromine-based initiator, in the presence of additional tetrabutylammonium chloride (TBACl), well-controlled polymerization of MA was achieved using 10–20 mol % of the added salt. However, further increasing the concentration of TBACl to 0.5 equiv increased the dispersity of polymers. This observation suggests that the possible transfer of Cl to the chain ends hinders the fast reactivation as opposed to the bromine-capped chains (Figure S26).

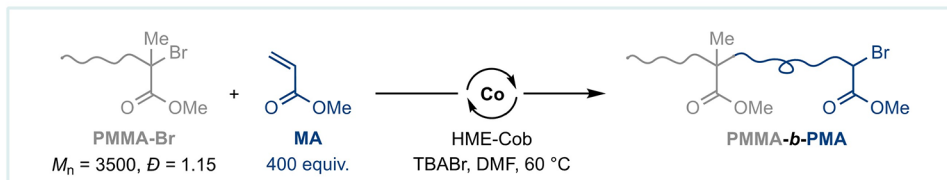
We used a bromine-capped poly(methyl methacrylate) (PMMA-Br) as a tertiary macroinitiator to further examine the initiation efficiency of the cobalt catalyst (Figure 7B). Polymerization of MA using the PMMA-Br macroinitiator showed near-quantitative initiation efficiencies (~98%). The GPC analysis of the copolymers showed only negligible residual macroinitiator while the formation of the block

## A — Alkyl halide initiators



[HME-Cob] = 0.05 equiv.						[HME-Cob] = 0.10 equiv.					
Initiator	Conv. (%)	$M_{n,\text{th}}$	$M_n$	$D$	$I_{\text{eff}} (\%)^a$	Initiator	Conv. (%)	$M_{n,\text{th}}$	$M_n$	$D$	$I_{\text{eff}} (\%)^a$
EBiB	50	8800	6600	1.20	134		65	11300	7900	1.13	143
BnBr	31	5600	5900	1.32	95		60	10500	7500	1.23	140
BPN	39	7000	4900	1.33	142		70	12000	7800	1.15	153
BAN	<2	600	5400	1.61	11		<2	600	5400	1.61	11
ECP	7	1400	4500	1.47	31		10	1800	3700	1.40	51

## B — Chain extension with a tertiary macroinitiator



HME-Cob (equiv.)	AIBN (equiv.)	Conv. (%)	$M_n$	$D$	$I_{\text{eff}} (\%)^b$
0.05	-	41	17000	1.32	97
0.10	-	61	21200	1.34	97
0.05	0.20	50	22200	1.37	98

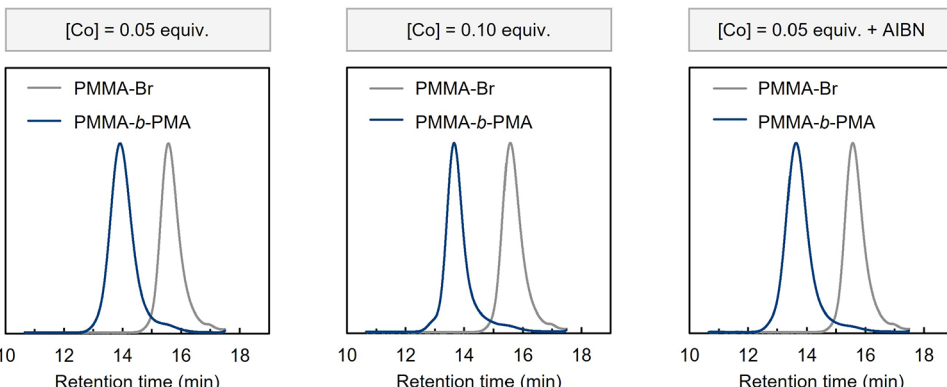


**Figure 7.** (A) Alkyl halide initiators examined in the polymerization of MA. Reaction conditions: [MA]/[R-X]/[HME-Cob]/[TBABr] = 200/1/0.05/0.10 (left panel) or 200/1/0.10/0.20 (right panel) in DMF at 60 °C; TBABr was used with ECP. <sup>a</sup> The initiator efficiency ( $I_{\text{eff}}$ ) was calculated based on the GPC analysis of polymers relative to polystyrene standards ( $I_{\text{eff}} = M_{n,\text{th}}/M_n$ ). (B) Polymerization of MA using a bromine-containing poly(methyl methacrylate) macroinitiator (PMMA-Br). <sup>b</sup> The initiator efficiency ( $I_{\text{eff}}$ ) was calculated based on the ratio of the area under the block copolymer peak to the total peak area including both the copolymer and the macroinitiator (shown in blue traces).

copolymer (PMMA-*b*-PMA) in a controlled manner was evident from the shift in the GPC traces to higher molecular weight.

## CONCLUSIONS

In summary, we developed a catalytic strategy to use a vitamin B<sub>12</sub>-derived cobalt complex to control radical polymerization reactions with alkyl halide initiators. The cobalt complex mediated the polymerization via an atom transfer mechanism establishing an equilibrium between active and dormant species, with Co<sup>II</sup> being the activator and Co<sup>III</sup>, in conjunction

with bromide anions, as the deactivator species. The polymerization efficiency of the cobalt complex differed according to its oxidation state (Co<sup>I</sup> vs Co<sup>II</sup>) during the initiation. The high reactivity of the Co<sup>I</sup> complex hampered polymerization control as opposed to the Co<sup>II</sup> complex that established the ATRP equilibrium and afforded polymers with controlled molecular weight properties. Through judicious design and development of reaction conditions to enhance the deactivation and enable catalyst regeneration, we established a fast and efficient strategy for cobalt-catalyzed atom transfer radical polymerization that provided high monomer conversions and well-controlled polymers using <5 mol % of the

catalyst. We anticipate that cobalt will offer new opportunities in designing ATRP catalysts and the synthesis of well-defined materials as well as advancing the development of bioinspired catalysis in controlled radical polymerization reactions.<sup>43</sup>

## ■ ASSOCIATED CONTENT

### SI Supporting Information

The Supporting Information is available free of charge at <https://pubs.acs.org/doi/10.1021/jacs.3c06783>.

Details of experimental procedures, molecular weight analysis, polymerization of MA initiated by Co<sup>II</sup>, kinetic studies, polymerizations using AIBN for catalyst regeneration, polymerizations at low catalyst concentrations, target degree of polymerization, polymerizations initiated by Co<sup>I</sup>, UV-vis spectroscopy, alkyl bromide initiators, effect of additional halide nature on polymerization control, cobalt-catalyzed ATRP using a tertiary macroinitiator, and NMR spectra (PDF)

## ■ AUTHOR INFORMATION

### Corresponding Author

Erin E. Stache – Department of Chemistry and Chemical Biology, Cornell University, Ithaca, New York 14853, United States; Present Address: Department of Chemistry, Princeton University, Princeton, New Jersey 08544, United States;  [0000-0002-4670-9117](https://orcid.org/0000-0002-4670-9117); Email: [estache@princeton.edu](mailto:estache@princeton.edu)

### Authors

Sajjad Dadashi-Silab – Department of Chemistry and Chemical Biology, Cornell University, Ithaca, New York 14853, United States; Present Address: Department of Chemistry, Princeton University, Princeton, New Jersey 08544, United States;  [0000-0002-4285-5846](https://orcid.org/0000-0002-4285-5846)

Cristina Preston-Herrera – Department of Chemistry and Chemical Biology, Cornell University, Ithaca, New York 14853, United States; Present Address: Department of Chemistry, Princeton University, Princeton, New Jersey 08544, United States

Complete contact information is available at: <https://pubs.acs.org/10.1021/jacs.3c06783>

### Notes

The authors declare no competing financial interest.

## ■ ACKNOWLEDGMENTS

We thank the Fors Group at Cornell University for using their GPC instrumentation. Financial support was provided by Cornell University. Acknowledgement is made to the donors of the American Chemical Society Petroleum Research Fund for partial support of this research. This work made use of the NMR Facility at Cornell University and was supported, in part, by the NSF under Award CHE-1531632. This work made use of the Cornell Center for Materials Research Facilities supported by the National Science Foundation under Award DMR-1719875.

## ■ REFERENCES

- Corrigan, N.; Jung, K.; Moad, G.; Hawker, C. J.; Matyjaszewski, K.; Boyer, C. Reversible-Deactivation Radical Polymerization (Controlled/Living Radical Polymerization): From Discovery to Materials Design and Applications. *Prog. Polym. Sci.* **2020**, *111*, No. 101311.
- Ouchi, M.; Sawamoto, M. 50th Anniversary Perspective: Metal-Catalyzed Living Radical Polymerization: Discovery and Perspective. *Macromolecules* **2017**, *50*, 2603–2614.
- Parkatzidis, K.; Wang, H. S.; Truong, N. P.; Anastasaki, A. Recent Developments and Future Challenges in Controlled Radical Polymerization: A 2020 Update. *Chem* **2020**, *6*, 1575–1588.
- di Lena, F.; Matyjaszewski, K. Transition Metal Catalysts for Controlled Radical Polymerization. *Prog. Polym. Sci.* **2010**, *35*, 959–1021.
- Poli, R. Relationship between One-Electron Transition-Metal Reactivity and Radical Polymerization Processes. *Angew. Chem., Int. Ed.* **2006**, *45*, 5058–5070.
- Shaver, M. P.; Allan, L. E. N.; Rzepa, H. S.; Gibson, V. C. Correlation of Metal Spin State with Catalytic Reactivity: Polymerizations Mediated by  $\alpha$ -Diimine–Iron Complexes. *Angew. Chem., Int. Ed.* **2006**, *45*, 1241–1244.
- Braunecker, W. A.; Brown, W. C.; Morelli, B. C.; Tang, W.; Poli, R.; Matyjaszewski, K. Origin of Activity in Cu-, Ru-, and Os-Mediated Radical Polymerization. *Macromolecules* **2007**, *40*, 8576–8585.
- Poli, R.; Allan, L. E. N.; Shaver, M. P. Iron-Mediated Reversible Deactivation Controlled Radical Polymerization. *Prog. Polym. Sci.* **2014**, *39*, 1827–1845.
- Wayland, B. B.; Poszmk, G.; Mukerjee, S. L.; Fryd, M. Living Radical Polymerization of Acrylates by Organocobalt Porphyrin Complexes. *J. Am. Chem. Soc.* **1994**, *116*, 7943–7944.
- Debuigne, A.; Poli, R.; Jérôme, C.; Jérôme, R.; Detrembleur, C. Overview of Cobalt-Mediated Radical Polymerization: Roots, State of the Art and Future Prospects. *Prog. Polym. Sci.* **2009**, *34*, 211–239.
- Peng, C.-H.; Yang, T.-Y.; Zhao, Y.; Fu, X. Reversible Deactivation Radical Polymerization Mediated by Cobalt Complexes: Recent Progress and Perspectives. *Org. Biomol. Chem.* **2014**, *12*, 8580–8587.
- Dadashi-Silab, S.; Stache, E. E. A Hydrometalation Initiation Mechanism via a Discrete Cobalt-Hydride for a Rapid and Controlled Radical Polymerization. *J. Am. Chem. Soc.* **2022**, *144*, 13311–13318.
- Allan, L. E. N.; Perry, M. R.; Shaver, M. P. Organometallic Mediated Radical Polymerization. *Prog. Polym. Sci.* **2012**, *37*, 127–156.
- Debuigne, A.; Jérôme, C.; Detrembleur, C. Organometallic-Mediated Radical Polymerization of ‘Less Activated Monomers’: Fundamentals, Challenges and Opportunities. *Polymer* **2017**, *115*, 285–307.
- Poli, R. A Journey into Metal–Carbon Bond Homolysis. *C. R. Chim.* **2021**, *24*, 147–175.
- Wang, J.-S.; Matyjaszewski, K. Controlled/“living” Radical Polymerization. Atom Transfer Radical Polymerization in the Presence of Transition-Metal Complexes. *J. Am. Chem. Soc.* **1995**, *117*, 5614–5615.
- Matyjaszewski, K.; Xia, J. Atom Transfer Radical Polymerization. *Chem. Rev.* **2001**, *101*, 2921–2990.
- Matyjaszewski, K. Atom Transfer Radical Polymerization (ATRP): Current Status and Future Perspectives. *Macromolecules* **2012**, *45*, 4015–4039.
- Lorandi, F.; Fantin, M.; Matyjaszewski, K. Atom Transfer Radical Polymerization: A Mechanistic Perspective. *J. Am. Chem. Soc.* **2022**, *144*, 15413–15430.
- Matyjaszewski, K. Advanced Materials by Atom Transfer Radical Polymerization. *Adv. Mater.* **2018**, *30*, No. 1706441.
- Fors, B. P.; Hawker, C. J. Control of a Living Radical Polymerization of Methacrylates by Light. *Angew. Chem., Int. Ed.* **2012**, *51*, 8850–8853.
- Treat, N. J.; Sprafke, H.; Kramer, J. W.; Clark, P. G.; Barton, B. E.; Read de Alaniz, J.; Fors, B. P.; Hawker, C. J. Metal-Free Atom Transfer Radical Polymerization. *J. Am. Chem. Soc.* **2014**, *136*, 16096–16101.
- Pan, X.; Fang, C.; Fantin, M.; Malhotra, N.; So, W. Y.; Peteanu, L. A.; Isse, A. A.; Gennaro, A.; Liu, P.; Matyjaszewski, K. Mechanism

of Photoinduced Metal-Free Atom Transfer Radical Polymerization: Experimental and Computational Studies. *J. Am. Chem. Soc.* **2016**, *138*, 2411–2425.

(24) Lorandi, F.; Matyjaszewski, K. Why Do We Need More Active ATRP Catalysts? *Isr. J. Chem.* **2020**, *60*, 108–123.

(25) Corbin, D. A.; Miyake, G. M. Photoinduced Organocatalyzed Atom Transfer Radical Polymerization (O-ATRP): Precision Polymer Synthesis Using Organic Photoredox Catalysis. *Chem. Rev.* **2022**, *122*, 1830–1874.

(26) Wang, B.; Zhuang, Y.; Luo, X.; Xu, S.; Zhou, X. Controlled/“Living” Radical Polymerization of MMA Catalyzed by Cobaltocene. *Macromolecules* **2003**, *36*, 9684–9686.

(27) Weiser, M.-S.; Mülhaupt, R. Cobalt(II) Octanoate and Cobalt(II) Perfluoroctanoate Catalyzed Atom Transfer Radical Polymerization of Styrene in Toluene and Fluorous Media—A Versatile Route to Catalyst Recycling and Oligomer Formation. *J. Polym. Sci., Part A: Polym. Chem.* **2005**, *43*, 3804–3813.

(28) Luo, X.; Zhuang, Y.; Zhao, X.; Zhang, M.; Xu, S.; Wang, B. Controlled/Living Radical Polymerization of Styrene Catalyzed by Cobaltocene. *Polymer* **2008**, *49*, 3457–3461.

(29) Luo, X.; Zhao, X.; Xu, S.; Wang, B. The Exo-Substituted H<sub>4</sub>-Cyclopentadiene CpCo(I) Complexes: A New Kind of ATRP Catalysts and the Actual Catalyst for the Cobaltocene-Catalyzed ATRP. *Polymer* **2009**, *50*, 796–801.

(30) Matsubara, K.; Matsumoto, M. Cobalt(I)-Mediated Living Radical Polymerization of Methyl Methacrylate. *J. Polym. Sci., Part A: Polym. Chem.* **2006**, *44*, 4222–4228.

(31) Wdowik, T.; Gryko, D. C–C Bond Forming Reactions Enabled by Vitamin B12—Opportunities and Challenges. *ACS Catal.* **2022**, *12*, 6517–6531.

(32) Sandford, C.; Fries, L. R.; Ball, T. E.; Minteer, S. D.; Sigman, M. S. Mechanistic Studies into the Oxidative Addition of Co(I) Complexes: Combining Electroanalytical Techniques with Parameterization. *J. Am. Chem. Soc.* **2019**, *141*, 18877–18889.

(33) Demarteau, J.; Debuigne, A.; Detrembleur, C. Organocobalt Complexes as Sources of Carbon-Centered Radicals for Organic and Polymer Chemistries. *Chem. Rev.* **2019**, *119*, 6906–6955.

(34) Hickey, D. P.; Sandford, C.; Rhodes, Z.; Gensch, T.; Fries, L. R.; Sigman, M. S.; Minteer, S. D. Investigating the Role of Ligand Electronics on Stabilizing Electrocatalytically Relevant Low-Valent Co(I) Intermediates. *J. Am. Chem. Soc.* **2019**, *141*, 1382–1392.

(35) Zhou, D.-L.; Walder, P.; Scheffold, R.; Walder, L. SN<sub>2</sub> or Electron Transfer?? A New Technique Discriminates the Mechanisms of Oxidative Addition of Alkyl Halides to Corrinato- and Porphyrinatocobalt(I). *Helv. Chim. Acta* **1992**, *75*, 995–1011.

(36) Giedyk, M.; Gryko, D. Vitamin B12: An Efficient Cobalt Catalyst for Sustainable Generation of Radical Species. *Chem. Catal.* **2022**, *2*, 1534–1548.

(37) Proinsias, K. Ó.; Jackowska, A.; Radzewicz, K.; Giedyk, M.; Gryko, D. Vitamin B12 Catalyzed Atom Transfer Radical Addition. *Org. Lett.* **2018**, *20*, 296–299.

(38) Ociepa, M.; Wierzba, A. J.; Turkowska, J.; Gryko, D. Polarity-Reversal Strategy for the Functionalization of Electrophilic Strained Molecules via Light-Driven Cobalt Catalysis. *J. Am. Chem. Soc.* **2020**, *142*, 5355–5361.

(39) Konkolewicz, D.; Magenau, A. J. D.; Averick, S. E.; Simakova, A.; He, H.; Matyjaszewski, K. ICAR ATRP with Ppm Cu Catalyst in Water. *Macromolecules* **2012**, *45*, 4461–4468.

(40) Matyjaszewski, K.; Jakubowski, W.; Min, K.; Tang, W.; Huang, J.; Braunecker, W. A.; Tsarevsky, N. V. Diminishing Catalyst Concentration in Atom Transfer Radical Polymerization with Reducing Agents. *Proc. Natl. Acad. Sci. U. S. A.* **2006**, *103*, 15309–15314.

(41) Toda, M. J.; Kozlowski, P. M.; Andruliów, T. Assessing Electronically Excited States of Cobalamins via Absorption Spectroscopy and Time-Dependent Density Functional Theory. In *Transition Metals in Coordination Environments: Computational Chemistry and Catalysis Viewpoints; Challenges and Advances in Computational Chemistry and Physics*; Broclawik, E.; Borowski, T.; Radoń, M., Eds.; Springer International Publishing: Cham, 2019; pp 219–258.

(42) Shimakoshi, H.; Shichijo, K.; Tominaga, S.; Hisaeda, Y.; Fujitsuka, M.; Majima, T. Catalytic Dehalogenation of Aryl Halides via Excited State Electron Transfer from the Co(I) State of B12 Complex. *Chem. Lett.* **2020**, *49*, 820–822.

(43) Rodriguez, K. J.; Gajewska, B.; Pollard, J.; Pellizzoni, M. M.; Fodor, C.; Bruns, N. Repurposing Biocatalysts to Control Radical Polymerizations. *ACS Macro Lett.* **2018**, *7*, 1111–1119.